RSC Advances

PAPER

View Article Online
View Journal | View Issue

Cite this: *RSC Adv.*, 2014, **4**, 56346

Crystallization induced layer-to-layer transitions in symmetric PEO-*b*-PLLA block copolymer with synchrotron simultaneous SAXS/WAXS investigations†

Feifei Xue,[a] Xuesi Chen,[b] Lijia An,[b] Sergio S. Funari[c] and Shichun Jiang*[a]

Received 26th August 2014
Accepted 22nd October 2014

DOI: 10.1039/c4ra09284h

www.rsc.org/advances

The time dependent hierarchical structures and crystallization behaviors of synthetic crystalline–crystalline symmetric diblock copolymer poly(ethylene oxide)-*b*-polylactide (PEO-*b*-PLLA) were investigated by DSC and synchrotron simultaneous small-angle/wide-angle X-ray scattering (SAXS/WAXS)measurements with various isothermal crystallization conditions. DSC measurements indicated that both blocks can crystallize and melt independently. Synchrotron SAXS/WAXS results showed that the structures and crystallization behaviors of PLLA and PEO blocks influence each other and the crystallization of both blocks could induce microphase separation into layer-layer structures, however, the crystalline structures of both blocks are not affected. It is assumed that the final structure of the crystalline–crystalline block copolymer is determined by the crystallization behaviors of the blocks rather than the glass transition temperature of the PLLA block and the theoretical microphase structure of the block copolymers.

Introduction

Phase separation and crystallization of polymers are of great technological importance due to the mechanical properties imparted, which ultimately result from the change in molecular conformation. Crystallization of block copolymer microdomains has a tremendous influence on the morphology, properties and applications of these materials. In semicrystalline block copolymers, the presence of a noncrystalline block enables modification of the mechanical and structural properties compared to a crystalline homopolymer, through introduction of rubbery or glassy component. Crystallization in homopolymers leads to an extended conformation, or kinetically controlled chain folding. In block copolymers, on the other hand, equilibrium chain folding occurred, and the equilibrium number of folds can be controlled by the size of the second noncrystallizable block. The most important crystallizable block copolymers are those containing polyethylene or poly(ethylene oxide). The melting temperature of PEO in block copolymers is generally lower than that of PEO homopolymer (melting temperature T = 76 °C for high molecular weight samples).[1]

The final solid-state structure in a block copolymer with at least one crystallizable block is the result of a complex interplay between microphase separation and crystallization.[2] Three general cases have been described in the literature depending on the relative location of the order–disorder transition temperature, TODT, the glass transition temperature (T_g), and the crystallization temperature (T_c). In the first case, amorphous-crystallizable diblock copolymer that form a homogeneous melt are considered, there TODT < T_c > T_g, and microphase separation is driven by crystallization because of the low T_g of the amorphous block as compared to T_c of the crystallizable block. In this case a lamellar morphology is obtained regardless of composition.[3–5] In the second case, weakly segregated systems with soft confinement have been described, where TODT > T_c > T_g. In this case the crystallization can provoke a "break-out" from the ordered melt morphology and crystallization can overwrite the morphological pattern of the melt with the possible formation of a lamellar structure, also once more regardless of composition.[5–12] The third general case is that of strongly segregated systems exhibiting hard confinement, where TODT > T_g > T_c. In this case, crystallization within spheres, cylinders or other types of confined morphologies has been observed for diblock and triblock copolymers with one glassy block, and the microphase segregated structure of the melt is generally preserved.[9,13–20]

[a]*School of Materials Science and Engineering, Tianjin University, Tianjin, 300072, P. R. China. E-mail: scjiang@tju.edu.cn*

[b]*State of Key Laboratory of Polymer Physics and Chemistry, Changchun Institute of Applied Chemistry, Chinese Academy of Sciences, Changchun, 130022, P. R. China*

[c]*HASYLAB at DESY, Notkestraße 85, D-22603 Hamburg, Germany*

† Electronic supplementary information (ESI) available. See DOI: 10.1039/c4ra09284h

Polymer crystallization was usually regarded as proceeding by heterogeneous nucleation, homogeneous nucleation, or self-nucleation. In bulk crystallizable polymers, nucleation is caused by heterogeneities (impurities, catalyst debris, or others). In block copolymers the nucleation depends on the continuity or isolation of the microdomains generated by phase segregation. Crystallization in continuous domains is induced by heterogeneous nucleation, because a percolation path for secondary crystallization exists. However, crystallization in isolated microdomains will either occur in a fractionated manner, where several crystallization exotherms are observed during a cooling DSC scan (the so-called fractionated crystallization phenomenon), or can only be induced by homogeneous nucleation at extreme supercooling. In block copolymers where the crystallizable component is confined into cylinders or spheres, the number density of isolated microdomains can be far greater than the number of available heterogeneities, thus creating ideal conditions for homogeneous nucleation.[9,13] When a crystallizable component is confined within a large number of small isolated microdomains, a substantial decrease in crystallinity compared to the corresponding homopolymers can sometimes be observed as a result of the larger supercoolings that are needed for crystallization and also topological restrictions due to confinement.[9] If the crystallizable block is confined into spherical, cylindrical or lamellar microdomains, an Avrami exponent of $n = 1$ has been observed and has been explained by homogeneous nucleation. However, in some puzzling cases Avrami exponents that are lower than 1 have been reported.[21,22]

There have been relatively few reports dealing with double crystalline diblock copolymers. In double crystalline diblock copolymers, the situation can be even more complicated, since the crystallization of one block may affect the crystallization and morphology of the other block. Recently, the reviews for the morphology and morphology formation of double crystalline block copolymers were reported and many differences can be found in the temperature range used for the study of the crystallization and melting process of PEO and PCL based AB diblock and ABA triblock copolymers.[23,24] In this report, we investigated the complex structure transitions of symmetrical crystalline–crystalline diblock copolymer induced by simultaneous microphase separation and crystallization *via* simultaneous synchrotron SAXS and WAXS measurements.

Experiment

Sample preparation and characterization

PEO-*b*-PLLA diblock copolymer was prepared by the ring-opening copolymerization of L-lactide (supplied by Purac) in the presence of monomethoxy-terminated poly (ethylene oxide) having one methyl group with a number average molecular weight of 5000 (supplied by Aldrich) catalyzed by stannous octoate ($Sn(Oct)_2$, 10 mol% relative to PEO) according to the method reported earlier.[25] Moreover, PLLA homopolymer was prepared by polymerization of LA catalyzed by $Sn(Oct)_2$ using alcohol as initiator. The molecular weight and the polydispersity, Mw/Mn, were determined by GPC (Waters 410). GPC traces indicated a single peak for homopolymer PLLA and a series of diblock copolymers PEO-*b*-PLLA. The copolymer composition was evaluated by ^{1}H NMR (Unity-400). Molecular weight of the PLLA block in the copolymer was determined from the copolymer composition on the basis of the PEO's molecular weight. Molecular weights and compositions of the PEO-*b*-PLLA diblock copolymers are shown in Table 1.

Table 1 Molecular weight and composition of PEO-*b*-PLLA diblock copolymer

		GPC		
Sample	^{1}H NMR (PEO/PLLA)	Mn	Mw	Mw/Mn
PEO_{5k}-*b*-$PLLA_{5k}$	5000/5070	25 700	31 100	1.21

A DSC experiment was performed with Perkin-Elmer DSC-7 differential scanning calorimeter for the observation of melting and crystallization of PEO-*b*-PLLA diblock copolymer. The sample was heated from 30 °C to 200 °C with a heating rate of 10 °C min^{-1} and then cooled with the same rate.

Synchrotron measurements

X-ray scattering experiments were performed by employing synchrotron radiation ($\lambda = 0.150$ nm) in the beamline A2 at HASYLAB (Hamburg, Germany) and beamline 1W2A (SAXS station) of Beijing Synchrotron Radiation Facility (Beijing, China) with $\lambda = 0.154$ nm. Two linear position-sensitive detectors were used simultaneously: one of them covering the approximate 2θ range from 10° to 30° and the other being set at 230 cm sample-detector distance (in the direction of the beam). Therefore, wide-angle X-ray scattering (WAXS), and small-angle X-ray scattering (SAXS) data are collected in the experimental setup: simultaneous WAXS/SAXS profiles are acquired.

Film samples, of about 50 mg, were covered by aluminum foil, to ensure homogeneous heating or cooling, and placed in the beamline with vacuum temperature controller for simultaneous SAXS/WAXS measurements. The symmetric block copolymer samples were annealed for 5 days in vacuum at 180 °C with *in situ* SAXS monitoring with the aid of a SWAXS twin camera produced by Hecus-Braun Co., Graz, Austria in Physikalisches Institut, Albert-Ludwigs-Universität, Freiburg, Germany. Heating or cooling experiments were performed at different rates from 1 to 40 °C min^{-1}. The WAXS data were used to monitor the crystallization behavior of the samples and the SAXS data were used to monitor the lamellar formation of the samples. The calibration of the spacings for the different detectors and positions was made as follows: the diffraction peaks of a crystalline PET sample were used for the WAXS detector and the different orders of the long spacing of rat tendon tail ($L = 65$ nm) were used for the SAXS detector.

Results and discussion

The melting temperatures of PEO (Mn = 5000) and PLLA (Mn = 5100) are 55.6 and 164.6 °C, respectively.[25] The DSC curves in Fig. 1 shows that for PEO_{5k}-*b*-$PLLA_{5k}$ there are two melting

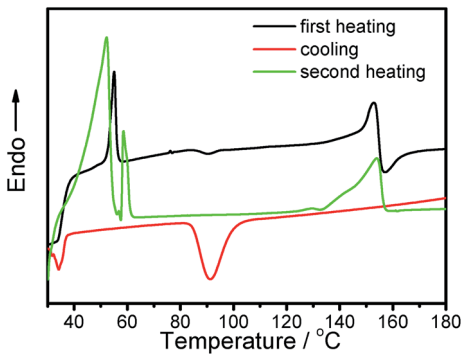

Fig. 1 DSC curves for PEO-*b*-PLLA block copolymer.

peaks during the first heating process and three melting peaks during the second heating process. The two melting peaks during the first heating may come from the crystallization of PEO and PLLA blocks in solution. The two melting peaks near 50 °C of the second heating process maybe due to the epitaxial crystallization of PEO on PLLA crystal or PLLA crystal induced crystallization of PEO in the block copolymer melting. One can also found two crystallization peaks during the cooling process of the block copolymer. DSC results indicate that the PEO and PLLA blocks can melt and crystallize independently in the diblock copolymer. Fig. 2 shows the WAXS results of PEO, PLLA and PEO_{5k}-*b*-$PLLA_{5k}$. It reveals that the crystals of the PEO (monoclinic) and PLLA (orthorhombic) in the block copolymer coexist independently and that there are no eutectic or mixed crystals containing both PEO and PLLA. The nanoscale structures of PEO, PLLA and symmetry diblock copolymer were investigated *via* SAXS, the results are shown in Fig. 3. It may indicated that all the structures of the homopolymers and the block copolymer are lamellae and the relationship of long space of the polymers are $L_{\text{coplymer}} > L_{\text{PLLA}} > L_{\text{PEO}}$.

To elucidate the nature of the multi-melting peaks of the symmetric double crystalline blocks copolymer of PEO-*b*-PLLA, the structure and the transition behavior of the copolymer were investigated by time-resolved synchrotron simultaneous WAXS/SAXS. The scattering patterns were collected in time frames of 10, 60 and 10 s for isothermal crystallization temperatures at 100, 50 and 40 °C, respectively.

Typical time-resolved SAXS and WAXS profiles obtained during isothermal crystallization of PEO_{5k}-*b*-$PLLA_{5k}$ at 40 °C after melting at 180 °C are shown in Fig. 4a and b, respectively. The SAXS results indicate that there is a formation of lamellar structure with decreasing long space and structural transition during the crystallization of the block copolymer quenched from melt. The WAXS results suggest that there is only the crystallization behavior of PEO block at the finished crystallization of PLLA block. The time evolution of the integrated intensity from the scattering maximum ($s = 0.042$ and $0.073\ \text{nm}^{-1}$) of SAXS profiles and strong reflections ((120) of PEO at $2\theta = 23.22°$ and (200)/(110) of PLLA at $2\theta = 19.04°/16.68°$, respectively) of WAXS profiles during the crystallization process are shown in Fig. 4a′ and b′. The results in Fig. 4b illustrates the change of the scattering intensity during the crystallization of PEO. However, the WAXS results in Fig. 2 indicate that there is no change of crystalline forms both for PEO and PLLA in the symmetric diblock copolymer.

Fig. 5 shows the time related Iq^2 *vs.* q obtained from SAXS results of this crystallization process. The maximum values of the scattering intensity are 1 and $\sqrt{3}$, which may indicates that there is a possible transition from lamellae to cylinders, then from cylinders to lamellae again or there are two kind of related lamellar structures with different spacings. In order to deduce the structural transition of this process, we analyzed the results of the symmetric diblock copolymer in Fig. 4b. From them, we knew that PLLA block almost finished crystallization before the temperature cooled to 40 °C from 180 °C. In other words, there is practically crystallization of PEO block at 40 °C in a hard environment of crystalline PLLA with the glass transition temperature higher than the crystallization temperature. In this case, it is impossible for the crystallization of PEO to over write the formed structure, and then to form new lamellae beyond the amorphous layer. Therefore, the conceivable structural transition is that PEO crystallizes from amorphous layer of the lamellar structure containing PLLA crystalline layer and the amorphous layer and then forms new lamellar structure containing PEO crystalline layer and amorphous layer. It is well known that the SAXS data obtained from the object with lamellar structure could be analyzed by the one-dimensional electron intensity correlation function $K(Z)$ defined by Strobl which can be derived from Fourier transition of scattering curve.[26]

$$K(Z) = \frac{1}{2\pi}\int_0^\infty I(s)s^2\cos(sZ)\mathrm{d}s \quad (1)$$

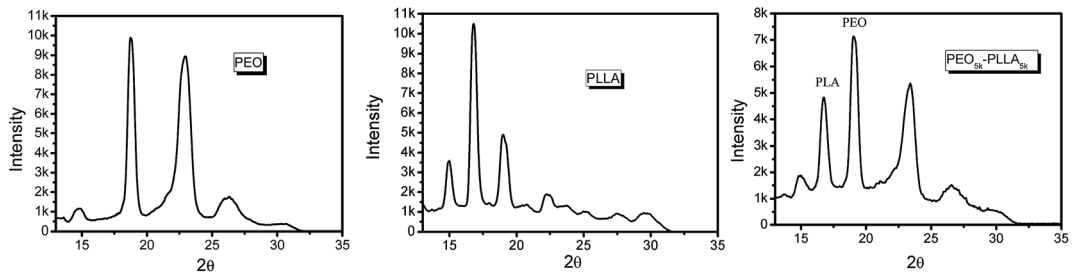

Fig. 2 WAXS patterns of PEO, PLLA and the PEO-*b*-PLLA block copolymer.

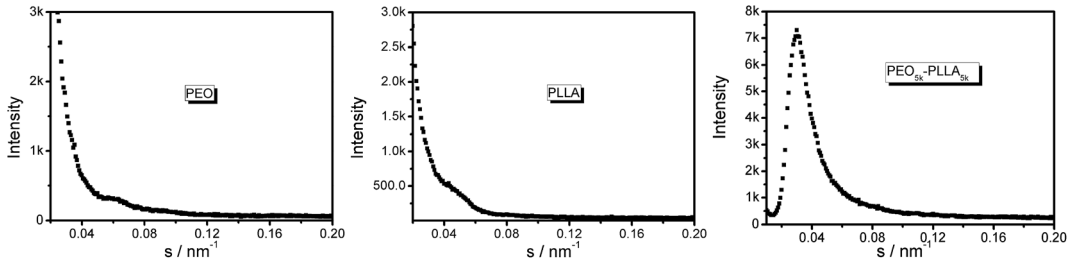

Fig. 3 SAXS patterns of PEO, PLLA and the PEO-*b*-PLLA block copolymer.

where $s = 2 \sin \theta/\lambda = q/2\pi$, the modulus of the momentum transfer vector q, and 2θ is the scattering angle. The calculated results are shown in Fig. 6 and the results showed that the long space for the initial and the final structures for this process are 20.3 nm and 13.3 nm for lamellar structures containing PLLA crystalline layer and PLLA/PEO crystalline layers, respectively. The crystalline thicknesses of the two stages are 8.2 nm and 7.6 nm. The calculated values confirm that the structural transition is from lamellae to lamellae during this process.

Fig. 7 shows SAXS and WAXS data obtained from the isothermal crystallization of the symmetric diblock copolymer at 100 °C. This relative low supercooling for PEO-*b*-PLLA block copolymer crystallization resulted in a relative low crystallization rate, allowing the possibility of the detailed examination of simultaneously collected SAXS and WAXS profiles. The SAXS results in Fig. 7a imply the long spacing is almost constant during the isothermal crystallization, and the WAXS results in Fig. 7b indicate that only PLLA block can crystallize in this experimental condition. The time for the first appearance of a

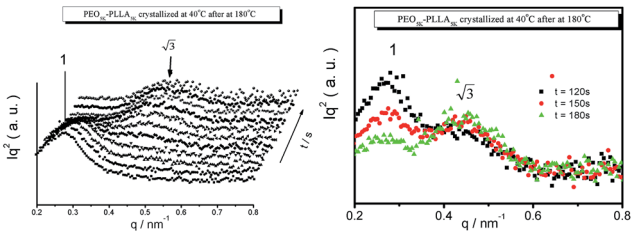

Fig. 5 Time related Is^2 *versus* s of PEO-*b*-PLLA crystallized at 40 °C during isothermal crystallization.

detectable scattering shoulder in the raw SAXS profile is almost the same as that when the crystalline reflections (WAXS) first become identifiable. This can be confirmed by comparing the time evolution of the integrated intensity from the scattering maximum ($s = 0.041$ nm^{-1}) of SAXS profiles and the strong (200)/(110) reflections of PLLA at $2\theta = 16.61$ of WAXS, shown in Fig. 7.

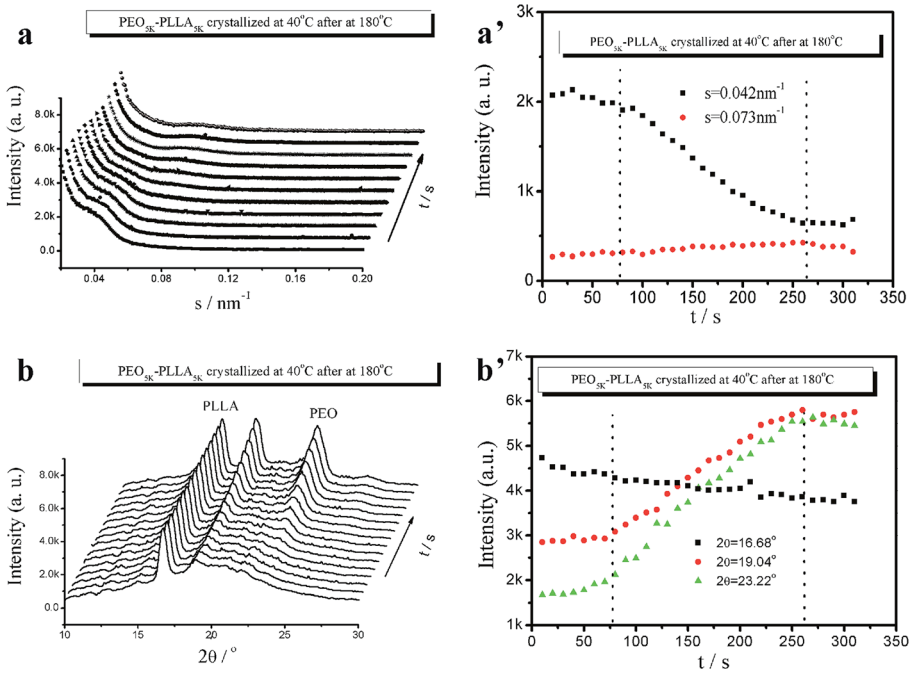

Fig. 4 Simultaneous profiles and the integrated intensity I_{int} as a function of time obtained from SAXS (a, a′) and WAXS (b, b′) measurements during isothermal crystallization of PEO-*b*-PLLA at 40 °C.

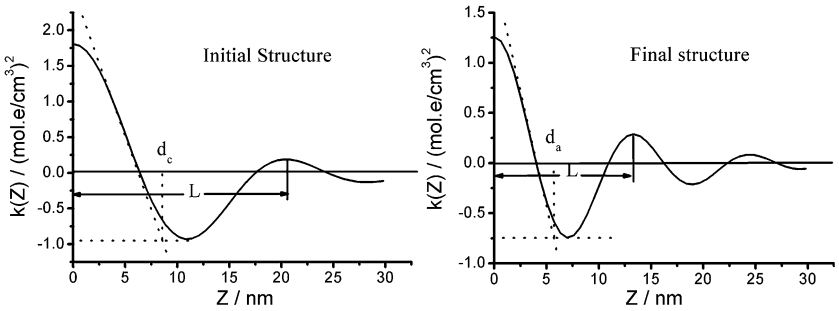

Fig. 6 Curves of experimental correlation function $K(Z)$ obtained for (a) initial structure and final structure of PEO-*b*-PLLA during isothermal crystallization at 40 °C after at 180 °C.

Fig. 8 shows the time-resolved SAXS and WAXS data of the isothermal crystallization of PEO_{5k}-*b*-$PLLA_{5k}$ at 40 °C, after it crystallized at 100 °C. The time evolution of the integrated intensity from the scattering peak ($s = 0.041$ and $0.069\ nm^{-1}$) of SAXS profiles and strong reflections ((120) of PEO at $2\theta = 23.22°$ and (200)/(110) of PLLA at $2\theta = 19.04°/16.75°$, respectively) of WAXS profiles are shown in Fig. 8a′ and b′. The results in Fig. 8b and b′ indicated that only the PEO block crystallized at 40 °C after it held at 100 °C for the isothermal crystallization of PLLA block as shown in Fig. 7. The lower supercooling for PEO-*b*-PLLA block copolymer resulted in a lower crystallization rate, allowing the more detailed examination of simultaneously collected SAXS and WAXS profiles. So we study the isothermal crystallization of the symmetric block copolymer at 50 °C after it cooling from 180 °C and 100 °C and compared with the results obtained at 40 °C. The selected time related SAXS and WAXS profiles of the time resolved crystallization process of the symmetric block copolymer at 50 °C cooling from 180 °C and 100 °C are shown in Fig. SI-1 and SI-2 (ESI†). It is worth noting that PLLA block have already crystallized completely before the

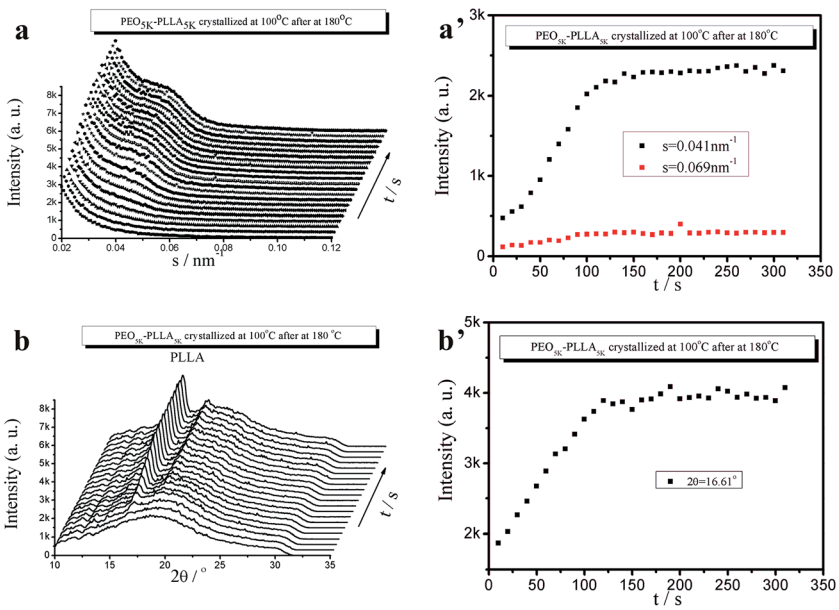

Fig. 7 Simultaneous profiles and the integrated intensity I_{int} as a function of time obtained from SAXS (a, a′) and WAXS (b, b′) measurements during isothermal crystallization of PEO-*b*-PLLA at 100 °C. It is reported that the peaks corresponding to the lamellar repeat were revealed in the supercooled melt (by SAXS) prior to the observation of three-dimensional crystal ordering (by WAXS), and the lag time ($t_{WAXS}-t_{SAXS}$) reduces with decreasing the crystallization temperature or increasing the degree of supercooling. Wang *et al.* reported the lag time is attributed to the detection limits of SAXS and WAXS. It is meaningless that only compare the first increase of the SAXS and WAXS intensities to confirm the appearance of initial crystalline phase because the detection limits of SAXS and WAXS are different. They considered that the crystallinity in the early stages is so low that the WAXS technique can not to detect it. But the crystallinity can be readily detectable by SAXS as long as the contrast between the constituting phases is sufficient and the length scale is within the detectable range.[27] However, the experiment data we obtained for PEO-*b*-PLLA and PEO-*b*-PCL block copolymers were not consistent with theirs as shown in Fig. 4 and (ref. 24). Our results obtained from crystalline–crystalline diblock copolymers *via* simultaneous SAXS/WAXS measurements indicate that SAXS and WAXS could detect polymer crystallization process with different scales simultaneously. In other words, the lamella and crystallite structural transitions of block copolymer with double crystalline blocks can be measured during the crystallization processes of the two blocks. The detail of the structural transitions can be investigated and analyzed from the crystallization of the block copolymers.

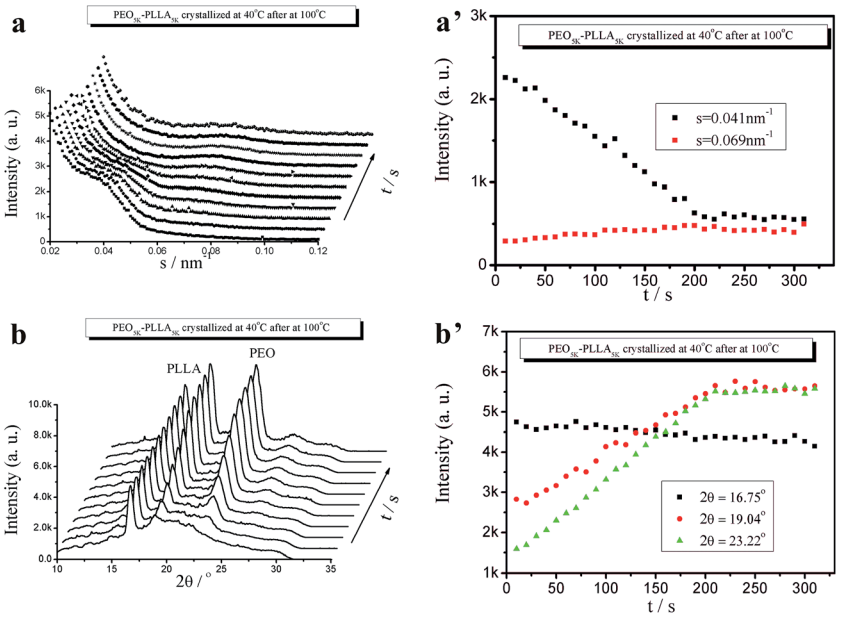

Fig. 8 Simultaneous profiles and the integrated intensity I_{int} as a function of time obtained from SAXS (a, a′) and WAXS (b, b′) measurements during isothermal crystallization of PEO-*b*-PLLA at 40 °C after at 100 °C.

crystallization of PEO block at 40 °C and 50 °C in PEO_{5k}-*b*-$PLLA_{5k}$ diblock copolymer, depending whether it crystallized from 180 °C or 100 °C as indicated in all of the related WAXS results.

Normally, the scattering intensity of SAXS obtained from polymer crystallization process increases with crystallization time. From the above SAXS patterns, we can find that is true for the diblock copolymer crystallized at 100 °C with the crystallization of PLLA. However, that is not the case for the PEO crystallization process in the diblock copolymer after the crystallization of PLLA block. A similar phenomenon was observed during the crystallization process of the crystalline–crystalline PEO-*b*-PCL diblock copolymer studied by simultaneous SAXS and WAXS technology.[28] The obtained SAXS and WAXS results indicate that there is a temperature dependent microphase separation and crystallization process in PEO-*b*-PLLA symmetric block copolymer, which is important to understand the mechanism of the structure formation and the final structure of such kinds of polymers. One can also find that all of the transitions of PEO-*b*-PLLA crystallization process take place at the same time for both of SAXS and WAXS for the block copolymer crystallized at 50 °C as shown in the related figures, which indicate both the nano- and micro-scale structure transformations relate to the PEO and PLLA block crystallization behavior and the block copolymer condensate structures.

It is a special phenomenon for the crystalline–crystalline diblock copolymer that one block crystallizes first with the simultaneous microphase separation, and then the other crystallizes. From the SAXS result in Fig. 4a, one can deduce that the maximum SAXS intensity is attributed to electron density difference of the domains induced by the microphase separation during the crystallization process. It is well known that the size of the crystalline lamella is the same magnitude of nano-scale as that of the microphase in the block copolymer and the long space includes PEO and PLLA layers. The obtained SAXS results indicate that the electron density difference of the two blocks first increases while one block crystallizes, then decreases when the other block crystallizes. For the crystalline–crystalline diblock copolymer with the glass transition temperature of one block higher than the crystallization temperature of the other block, the structural transitions must be complicated during the crystallization from melt. The SAXS results indicate a compatible system before the crystallization of PLLA and then hard confined crystallization of PEO in crystalline and glassy amorphous of PLLA with the sample quenched to room temperature from melt. Because the PLLA crystallization simultaneously induced microphase separation of the block copolymer, we deduced that the relationship of the transition temperatures of the block copolymer is $T_{c,PLA} \approx T_{ODT,COP} > T_{g,PLLA} > T_{c,PEO}$. The structural transitions of the symmetric diblock copolymer can be easily obtained according to this relation.

A remarkable property of block copolymers is the ability to self-assemble into a variety of ordered structures with nanoscale periodicities due to microphase separation. These ordered structures can be controlled by temperature, the polymerization degree or the composition of the block copolymer. Microphase separation is driven by the enthalpy of demixing of the constituent component of the block copolymers, whilst macrophase separation is prevented by the chemical connectivity of the block. For a diblock copolymer, the volume fraction of one component controls which ordered structures are accessed beneath the order–disorder transition. Symmetric block copolymers can form a lamellar phase, with alternating layers of the constituent blocks. Following the crystallization kinetics and the temperature dependence of the long spacing, we considered

that the crystallized morphology of PEO_{5k}-*b*-$PLLA_{5k}$ block copolymer is overall lamellar, as other groups suggested.[29,30] The integrated intensity obeys the following equation:[26]

$$I_{\text{int}} = \int_{q_2}^{q_1} I(q)q^2 \mathrm{d}q \propto \phi_a \phi_c (\rho_a - \rho_c)^2 \quad (2)$$

In eqn (2), the integrated intensity I_{int} is proportional to the product of volume fraction for the crystalline and amorphous phases (ϕ_c,ϕ_a) and the electron density difference $(\rho_a - \rho_c)^2$. It is well known that the crystallinity of half crystalline polymers is usually lower than 50%, and the maximum of $\phi_a\phi_c(\rho_a - \rho_c)^2$ usually appears at crystallinity that is higher than 60%, so ϕ_a-$\phi_c(\rho_a - \rho_c)^2$ normally increases with crystallization time during the isothermal polymer crystallization process. Therefore, I_{int} should increase with time when polymer crystallizes from melt. In our experiment, according to the results obtained for the isothermal crystallization of the symmetry diblock copolymer, the integrated intensity I_{int} obtained from SAXS not always increases with time during the crystallization process. It indicates that the scattering intensity I_{int} is controlled by the crystallization and microphase separation behaviors of PEO and PLLA blocks rather than the crystalline and amorphous phase as that in homopolymers. For PEO_{5k}-*b*-$PLLA_{5k}$ crystalline–crystalline symmetric diblock copolymers, there is layer structure at ordered melt due to the simultaneous microphase separation induced by the crystallization of PLLA block. In this system there are at least four phases: crystal PEO, crystal PLLA, amorphous PEO and amorphous PLLA. We could not detect whether the melt structure of the block copolymer is ordered or not before any of the blocks crystallized because the density and the electron density between PEO and PLLA melt are almost the same, and the electron density difference between amorphous (and crystal) PEO and amorphous (and crystal) PLLA is too small to be detected,[30] *i.e.*, the following relations can be obtained

$$\rho_{\text{PEO,m}} \approx \rho_{\text{PLLA,m}}, \quad (3)$$

and

$$\rho_{\text{PEO,ed}} \approx \rho_{\text{PLLA,ed}}, \quad (4)$$

where $\rho_{\text{PEO,m}}$ and $\rho_{\text{PLLA,m}}$ are the melt density of PEO and PLLA, $\rho_{\text{PEO,ed}}$ and $\rho_{\text{PLLA,ed}}$ are the electron density of PEO and PLLA. There would be two phases with the crystallization of PLLA block and three phases with both of the blocks crystallization, if PEO and PLLA blocks are miscible in melt.

According to eqn (2) and (4), we can obtain the electron density difference between PEO and PLLA block during the crystallization process:

$$(\rho_c - \rho_a)^2 \approx (\rho_{\text{PEO}} - \rho_{\text{PLLA}})^2, \quad (5)$$

where ρ_{PEO} and ρ_{PLLA} are the electron density of PEO phase and PLLA phase, respectively. In the diblock copolymer, the crystallization begins by microphase separation, *i.e.*, PEO phase and PLLA phase. The volume fraction of the two phases are ϕ_{PEO} and ϕ_{PLLA}. Then we can simplify eqn (1) as

$$I_{\text{int}} \propto \phi_{\text{PEO}}\phi_{\text{PLLA}}(\rho_{\text{PEO}} - \rho_{\text{PLLA}})^2, \quad (6)$$

i.e., the integrated intensity I_{int} is proportional to the product of volume fraction for the PEO and PLLA phase (ϕ_{PEO} and ϕ_{PLLA} are constant in our experiment) and the electron density difference $(\rho_{\text{PEO}} - \rho_{\text{PLLA}})^2$ in PEO_{5k}-*b*-$PLLA_{5k}$ crystallization process. Because PLLA block crystallized first and then PEO crystallized, for PEO-PLLA cooled from melt to 40 °C and crystallized at 40 °C, the electron density difference $(\rho_{\text{PEO}} - \rho_{\text{PLLA}})^2$ increased first for PLLA block crystallization during the cooling process and then decreased with PEO block crystallization. It is consistent with the data showed in Fig. 4a obtained from PEO block crystallization. The interrelated transitions seen in Fig. 4a and a′ can be interpreted with $I_{\text{int}} \propto \phi_{\text{PEO}}\phi_{\text{PLLA}}(\rho_{\text{PEO}} - \rho_{\text{PLLA}})^2$. I_{int} is determined by the crystallization rate of PLLA and PEO.

Our observations on the block copolymer may be of interest for the results from the polymer crystallization process measured by simultaneous SAXS and WAXS.[31,32] The results in Fig. 4 show that the simultaneous SAXS and WAXS can detect the transition of crystallization in two size domains at the same time, which implies that the SAXS and WAXS could detect the same fraction of crystallinity at the same time. The SAXS peak originated from electronic density fluctuations of two phases on the range between 5–100 nm, while WAXS crystalline peaks were brought about by three-dimensional crystal ordering on the range between 0.2–1 nm. The earlier appearance of the SAXS peak than the WAXS crystalline peaks suggested that density fluctuations occurred prior to the crystallization during polymer crystallization.

More information about structural parameters such as the average lamellar thickness and the long spacing can be obtained according to eqn (1). As an example, the derived typical one-dimensional election intensity correction function $K(z)$ of the lamellar structures for PEO and PEO_{5k}-*b*-$PLLA_{5k}$ are demonstrated in Fig. 6. From the well-known "self-correction triangle" which reflects the electron-density correction within a lamella, one can directly estimate various structural parameters of the solid state for PEO and PEO_{5k}-*b*-$PLLA_{5k}$ by making use of some general properties of the correlation function. The invariant Q is the value of $K(z)$ at $z = 0$ which is also evaluated by extrapolating the straight-line section of the self-correlation region to the $K(z)$ axis (see Fig. 6). Its physical meaning is the mean-square electron density fluctuation. From the curvature of the straight-line segment in the central section of $K(z)$, the thickness of the transition layer d_{tr} could be estimated. According to Strobl, the thickness of the transition zone can be obtained directly from the curvature of $K(z)$. The long period L could be determined from the position of the first maximum in the correlation function. The average lamellar thickness $\bar{d}$ can be obtained by the cross point of the baseline with the sloping line of the "self-correlation triangle". The calculated long period and lamellar thickness for PEO, PLLA and PEO_{5k}-*b*-$PLLA_{5k}$ are shown in Table 2. The reduction in the long period and the lamellar thickness is due to the difference between the amorphous and the crystalline volumes in the block copolymer.

The symmetric block copolymer has been annealed for 5 days in vacuum at 180 °C with *in situ* SAXS monitoring. The

Table 2 Time related structure parameters of the block copolymer with different crystallization process[a]

Crystallization process	T (s)	L (nm)	Lc (nm)	Ltr (nm)
The sample crystallized at 40 °C after cooling from 180 °C	0	20.9	8.9	3.2
	80	20.2	9.2	2.9
	250	13.0	7.1	1.9
	Final	13.0	7.0	1.8
The sample crystallized at 100 °C after cooling from 180 °C	0	20.9	10.2	3.3
	20	20.9	10.2	3.2
	40	21.6	10.3	3.0
	60	22.2	10.3	3.0
	80	22.2	9.9	3.1
	110	22.2	9.9	3.0
The sample crystallized at 40 °C after crystallized at 100 °C	0	23.5	10.1	3.3
	20	23.5	10.1	3.8
	200	14.0	8.1	2.0
	300	14.0	8.1	2.1
The sample crystallized at 50 °C after cooling from 180 °C	0	20.9	9.1	2.7
	120	20.9	9.1	2.8
	3000	21.6	9.3	3.1
The sample crystallized at 50 °C after crystallized at 100 °C	0	23.5	10.3	3.4
	20	23.5	10.3	3.4
	1500	22.2	9.6	2.8
	4920	22.8	10.0	3.3

[a] T is isothermal crystallization time, L is lamellar long spacing, L_c is the lamellar thickness, and L_{tr} is the thickness of transition layer.

annealed SAXS results show no scattering peak. The SAXS intensity patterns of the PEO_{5k}-*b*-$PLLA_{5k}$ block copolymer during isothermal crystallization at 100 °C show no transitions before crystallized. It indicates that SAXS can not estimate whether PEO and PLLA are miscible or microphase separated before the diblock copolymer crystallized because of the too small density contrast between amorphous PEO and PLLA. However, the structural parameters of the copolymer and DSC result indicate PEO_{5k}-*b*-$PLLA_{5k}$ block copolymer has a sandwich structure and the block copolymer confined crystallized from melt. Fig. 9 schematically shows the possible step-crystallization behaviors of PEO_{5k}-*b*-$PLLA_{5k}$ block copolymer. The PLLA block crystallizes first with simultaneous microphase separation at 100 °C from melt in block copolymer (Fig. 9b) and then the PEO block crystallizes with the second simultaneous microphase separation at 40 °C or 50 °C after isothermal crystallization at 100 °C (Fig. 9c).

The interaction between microphase separation and crystallization results in a complicated final structure of the PEO_{5k}-*b*-$PLLA_{5k}$ block copolymer. The glass transition temperature of PEO is lower than the isothermal crystallization temperatures (at 40 °C and 50 °C). For the present symmetric block copolymer, weakly segregated system with soft confinement has been described, where the order–disorder transition temperature is higher than the crystallization temperatures and the crystallization temperatures of PLLA block are higher than the glass transition temperatures of both of the blocks. In this case the crystallization can provoke a "break-out" from the ordered melt morphology and crystallization can overwrite the morphological pattern of the melt with the possible formation of a lamellar structure, regardless of composition.[5,6,9] The melt morphology of symmetric block copolymers is lamellae driven by microphase separation. The results in Table 2 indicate the soft confined crystallization behavior of the crystalline–crystalline diblock copolymer. For each of the lamellae, crystalline and amorphous of each block are included, and the transition layer includes both PEO and PLLA.

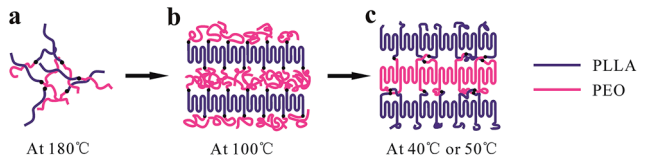

Fig. 9 Possible schematic diagrams of the structure transitions of the isothermal crystallization of PEO-*b*-PLLA at different temperatures.

Conclusions

We have discussed the isothermal crystallization behavior for symmetric PEO-*b*-PLLA diblock copolymers by measuring time-resolved synchrotron simultaneous SAXS/WAXS, from which detailed structural evolution process has been deduced and the crystallization behavior has been investigated. The SAXS/WAXS results show that the structure of PEO-*b*-PLLA block copolymer transits from lamella to lamella during the crystallization of PLLA and PEO blocks at different crystallization temperatures, which is probably a special phenomenon of copolymers with crystalline–crystalline blocks. The transitions of PEO-*b*-PLLA diblock copolymer during molten crystallization could be detected from the layer scale to crystal scale by SAXS and WAXS at the same time. In addition, the time-resolved I_{int} is proportional to the product of volume fraction for the PEO and PLLA phases (ϕ_{PEO},ϕ_{PLLA}) and the scattering contrast due to the

electron density difference$(\rho_{PEO} - \rho_{PLLA})^2$ during the block copolymer crystallization.

Acknowledgements

This work is supported by the National Natural Science Foundation of China (21374077, 20974077, 20620120105). Synchrotron experiments at Beam line A2 were supported by HASYLAB project (II20070004, II20090111).

References

1 I. W. Hamley, *The physics of block copolymers*, Oxford University Press, New York, 1998.
2 J. Albuerne, L. Marquez, A. Müller, J. Raquez, P. Degée, P. Dubois, V. Castelletto and I. Hamley, *Macromolecules*, 2003, **36**, 1633–1644.
3 P. Rangarajan, R. A. Register, D. H. Adamson, L. J. Fetters, W. Bras, S. Naylor and A. J. Ryan, *Macromolecules*, 1995, **28**, 1422–1428.
4 A. Ryan, I. Hamley, W. Bras and F. Bates, *Macromolecules*, 1995, **28**, 3860–3868.
5 P. Richardson, R. Richards, D. Blundell, W. MacDonald and P. Mills, *Polymer*, 1995, **36**, 3059–3069.
6 I. W. Hamley, J. P. A. Fairclough, N. J. Terrill, A. J. Ryan, P. M. Lipic, F. S. Bates and E. Towns-Andrews, *Macromolecules*, 1996, **29**, 8835–8843.
7 S. Nojima, K. Kato, S. Yamamoto and T. Ashida, *Macromolecules*, 1992, **25**, 2237–2242.
8 A. J. Ryan, J. P. A. Fairclough, I. W. Hamley, S.-M. Mai and C. Booth, *Macromolecules*, 1997, **30**, 1723–1727.
9 Y.-L. Loo, R. A. Register and A. J. Ryan, *Macromolecules*, 2002, **35**, 2365–2374.
10 V. T. Lipik, J. F. Kong, S. Chattopadhyay, L. K. Widjaja, S. S. Liow, S. S. Venkatraman and M. J. Abadie, *Acta Biomater.*, 2010, **6**, 4261–4270.
11 I. Hamley, V. Castelletto, R. V. Castillo, A. J. Müller, C. Martin, E. Pollet and P. Dubois, *Macromolecules*, 2005, **38**, 463–472.
12 S. Huang, S. Jiang, L. An and X. Chen, *J. Polym. Sci., Part B: Polym. Phys.*, 2008, **46**, 1400–1411.
13 A. Müller, V. Balsamo, M. Arnal, T. Jakob, H. Schmalz and V. Abetz, *Macromolecules*, 2002, **35**, 3048–3058.
14 S. Nojima, M. Toei, S. Hara, S. Tanimoto and S. Sasaki, *Polymer*, 2002, **43**, 4087–4090.
15 G. Reiter, G. Castelein, J.-U. Sommer, A. Röttele and T. Thurn-Albrecht, *Phys. Rev. Lett.*, 2001, **87**, 226101.
16 M. Arnal, V. Balsamo, F. Lopez-Carrasquero, J. Contreras, M. Carrillo, H. Schmalz, V. Abetz, E. Laredo and A. Müller, *Macromolecules*, 2001, **34**, 7973–7982.
17 L. Zhu, B. R. Mimnaugh, Q. Ge, R. P. Quirk, S. Z. Cheng, E. L. Thomas, B. Lotz, B. S. Hsiao, F. Yeh and L. Liu, *Polymer*, 2001, **42**, 9121–9131.
18 P. Weimann, D. Hajduk, C. Chu, K. Chaffin, J. Brodil and F. Bates, *J. Polym. Sci., Part B: Polym. Phys.*, 1999, **37**, 2053–2068.
19 H.-L. Chen, J.-C. Wu, T.-L. Lin and J. Lin, *Macromolecules*, 2001, **34**, 6936–6944.
20 Y.-L. Loo, R. A. Register, A. J. Ryan and G. T. Dee, *Macromolecules*, 2001, **34**, 8968–8977.
21 B. Lotz and A. Kovacs, *ACS Polym. Prepr.*, 1969, **10**, 820–825.
22 T. Shiomi, H. Tsukada, H. Takeshita, K. Takenaka and Y. Tezuka, *Polymer*, 2001, **42**, 4997–5004.
23 A. J. Müller, M. L. Arnal and V. Balsamo, in *Progress in understanding of polymer crystallization*, Springer, 2007, pp. 229–259.
24 R. Castillo and A. Müller, *Prog. Polym. Sci.*, 2009, **34**, 516–560.
25 J. Sun, Z. Hong, L. Yang, Z. Tang, X. Chen and X. Jing, *Polymer*, 2004, **45**, 5969–5977.
26 G. Strobl, M. Schneider and I. Voigt-Martin, *J. Polym. Sci., Polym. Phys. Ed.*, 1980, **18**, 1361–1381.
27 Z.-G. Wang, B. S. Hsiao, E. B. Sirota, P. Agarwal and S. Srinivas, *Macromolecules*, 2000, **33**, 978–989.
28 S. Jiang, C. He, Y. Men, X. Chen, L. An, S. S. Funari and C.-M. Chan, *Eur. Phys. J. E. Soft Matter*, 2008, **27**, 357–364.
29 B. Bogdanov, A. Vidts, E. Schacht and H. Berghmans, *Macromolecules*, 1999, **32**, 726–731.
30 L. Li, F. Meng, Z. Zhong, D. Byelov, W. H. de Jeu and J. Feijen, *J. Chem. Phys.*, 2007, **126**, 024904.
31 M. Imai, K. Kaji, T. Kanaya and Y. Sakai, *Phys. Rev. B: Condens. Matter Mater. Phys.*, 1995, **52**, 12696.
32 N. J. Terrill, P. A. Fairclough, E. Towns-Andrews, B. U. Komanschek, R. J. Young and A. J. Ryan, *Polymer*, 1998, **39**, 2381–2385.

